Pharmacologic targeting of the p62 ZZ domain enhances both anti-tumor and bone-anabolic effects of bortezomib in multiple myeloma

Silvia Marino,[1] Daniela N. Petrusca,[1] Ryan T. Bishop,[2] Judith L. Anderson,[1] Hayley M. Sabol,[3] Cody Ashby,[4] Justin H. Layer,[1] Annamaria Cesarano,[1] Utpal P. Davé,[1] Fabiana Perna,[1] Jesus Delgado-Calle,[3,5] John M. Chirgwin[1,6] and G. David Roodman[1,6]

[1]Department of Medicine, Division of Hematology/Oncology, Indiana University School of Medicine, Indianapolis, IN; [2]Department of Tumor Biology, H. Lee Moffitt Cancer Research Center and Institute, Tampa, FL; [3]Department of Physiology and Cell Biology, University of Arkansas for Medical Sciences, Little Rock, AR; [4]Department of Biomedical Informatics, University of Arkansas for Medical Sciences, Little Rock, AR; [5]Winthrop P. Rockefeller Cancer Institute, University of Arkansas for Medical Sciences, Little Rock, AR and [6]Research Service, Roudebush Veterans Administration Medical Center, Indianapolis, IN, USA

Correspondence: S. Marino
SMarino@uams.edu

Received: July 10, 2023.
Accepted: November 7, 2023.
Early view: November 16, 2023.

https://doi.org/10.3324/haematol.2023.283787

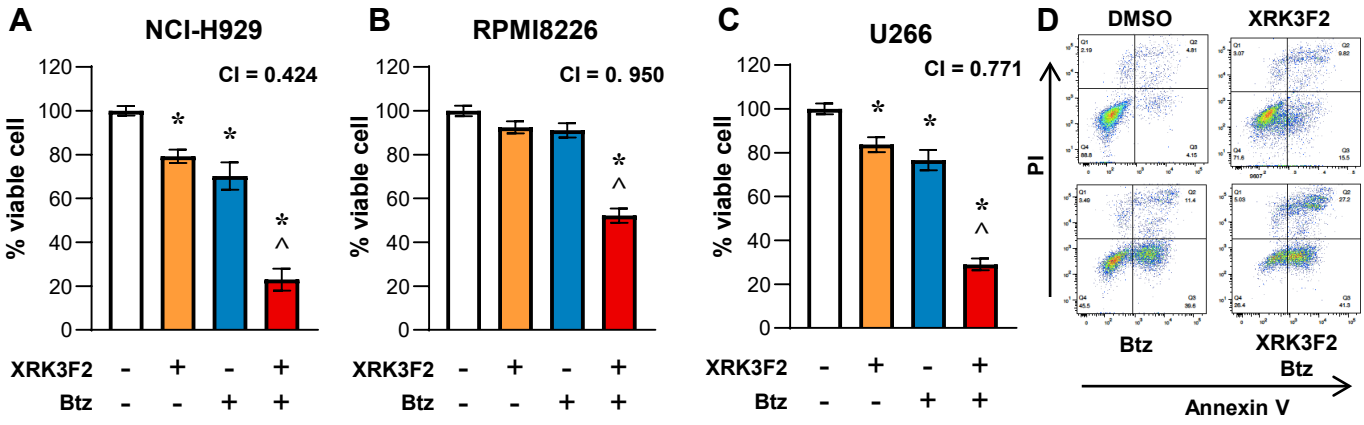

Supplementary Fig. 1. **Combination of low doses of XRK3F2 and Bortezomib synergistically increases MM cell death *in vitro*. A** NCI-H929, **B** RPMI-8226, **C** U266, and **D** MM1.S; cells were treated for 24h (or 6h (**D**)) with XRK3F2 (5μM), Btz (3nM), or combined XRK3F2-Btz (5μM/3nM). MM cell viability was evaluated by alamarBlue assay and is reported as percent vs. DMSO vehicle control. CI of less than 1 indicates synergy. MM cell death was evaluated by (**D**) Annexin V/propidium iodide (PI) staining in monoculture after 6h of treatment. Data are presented as bars, means±SD (n=4-6/group). *p<0.05 vs vehicle, ^p<0.05 vs XRK3F2 or Btz alone by one-way ANOVA with post hoc Tukey's correction.

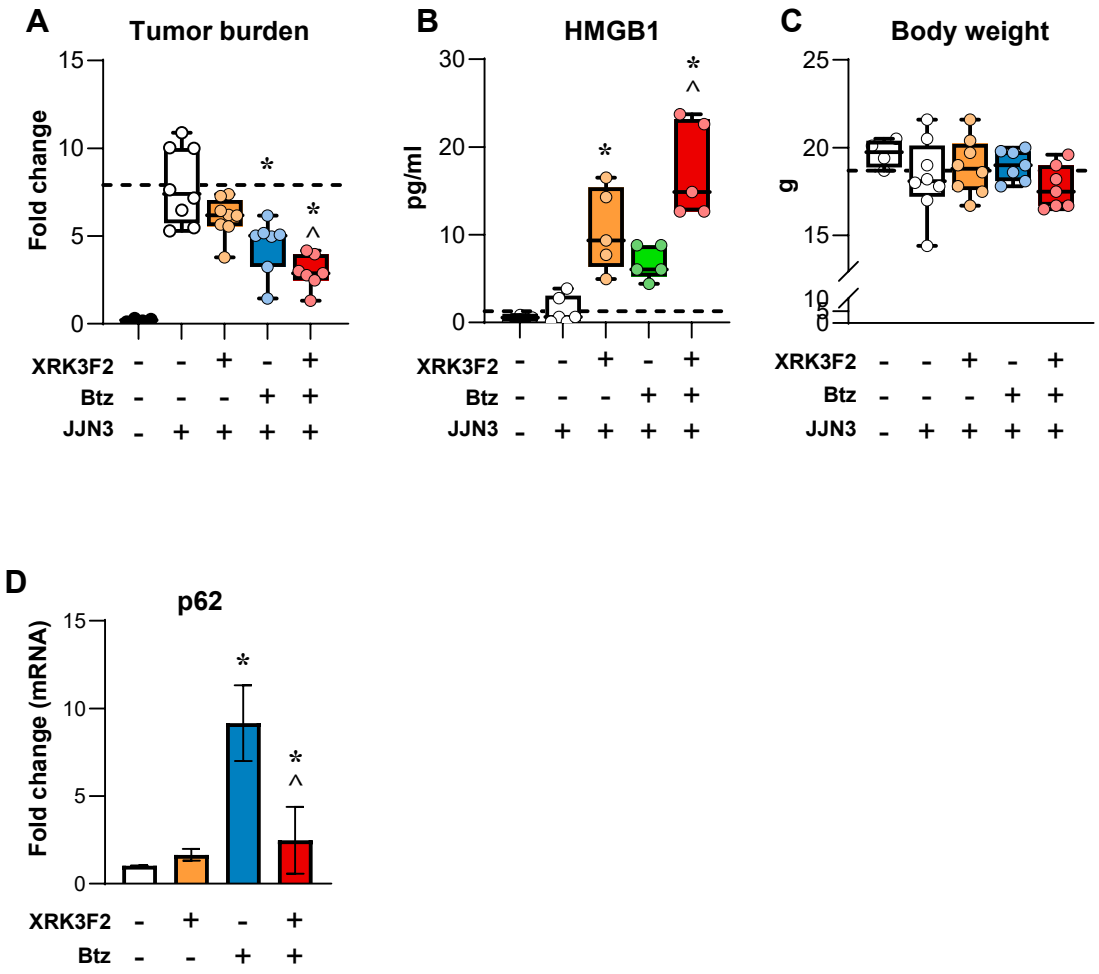

Supplementary Fig. 2. **XRK3F2 plus Bortezomib combination suppresses human JJN3 MM cell growth *in vivo*.** Serum level of **A** JJN3 tumor biomarker human Kappa light chain and **B** human high-mobility group box 1 protein (HMGB1) and **C** body weight after *in vivo* treatment with XRK3F2 (27mg/kg/5xweek), Btz (0.25mg/kg/2xweek) or XRK3F2-Btz combination (27mg/kg/5xweek plus 0.25mg/kg/2xweek, respectively) n=7-10 mice/group. Data are presented as box & whiskers plots where each dot represents a mouse. *p<0.05 vs JJN3-vehicle and ^p<0.05 vs JJN3-XRK3F2 or Btz alone by one-way ANOVA with post hoc Dunnet's correction. The horizontal dotted line indicates the mean value for vehicle-treated mice bearing JJN3 tumors. **D** Quantitative RT-PCR analysis of p62 mRNA in MM.1S cells treated with XRK3F2 (5μM), Btz (3nM), or combined XRK3F2-Btz (5μM/3nM) for 12 hours. Data are presented as bars, means±SD (n=4-6/group). *p<0.05 vs vehicle, ^p<0.05 vs XRK3F2 or Btz alone by one-way ANOVA with post hoc Tukey's correction.

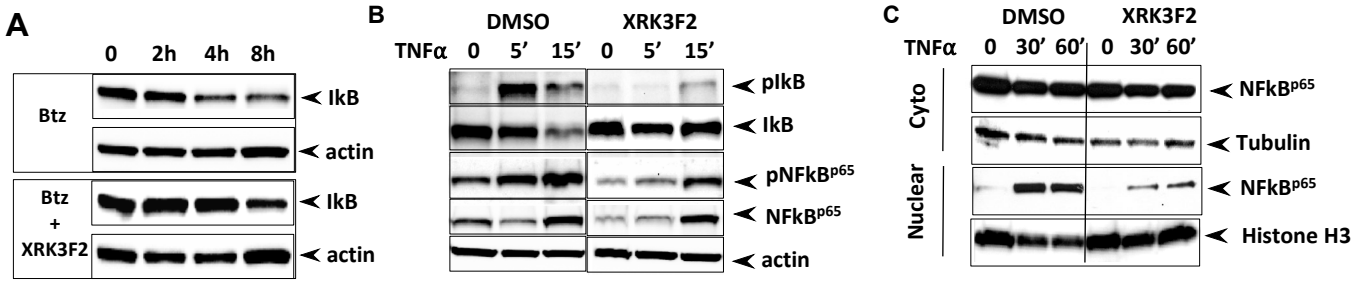

Supplementary Fig 3. XRK3F2 blocks Bortezomib-induced activation of NFκB.
A MM.1S cells were treated with Btz (10nM) in the presence or absence of XRK3F2 (10μM) for the indicated time points after which IκBα expression levels were determined by immunoblot analysis. **B** and **C** MM.1S cells were pre-treated with either DMSO or XRK3F2 (10 μM) for 2h and then stimulated with TNFα (10ng/ml) for either 5, 15 minutes (**B**) or 30 and 60 minutes (**C**) after which expression levels of phosphorylated IκBα and $NFkB^{p65}$ (**B**) or nuclear translocation of $NFκB^{p65}$ (**C**) were determined by immunoblot analysis.

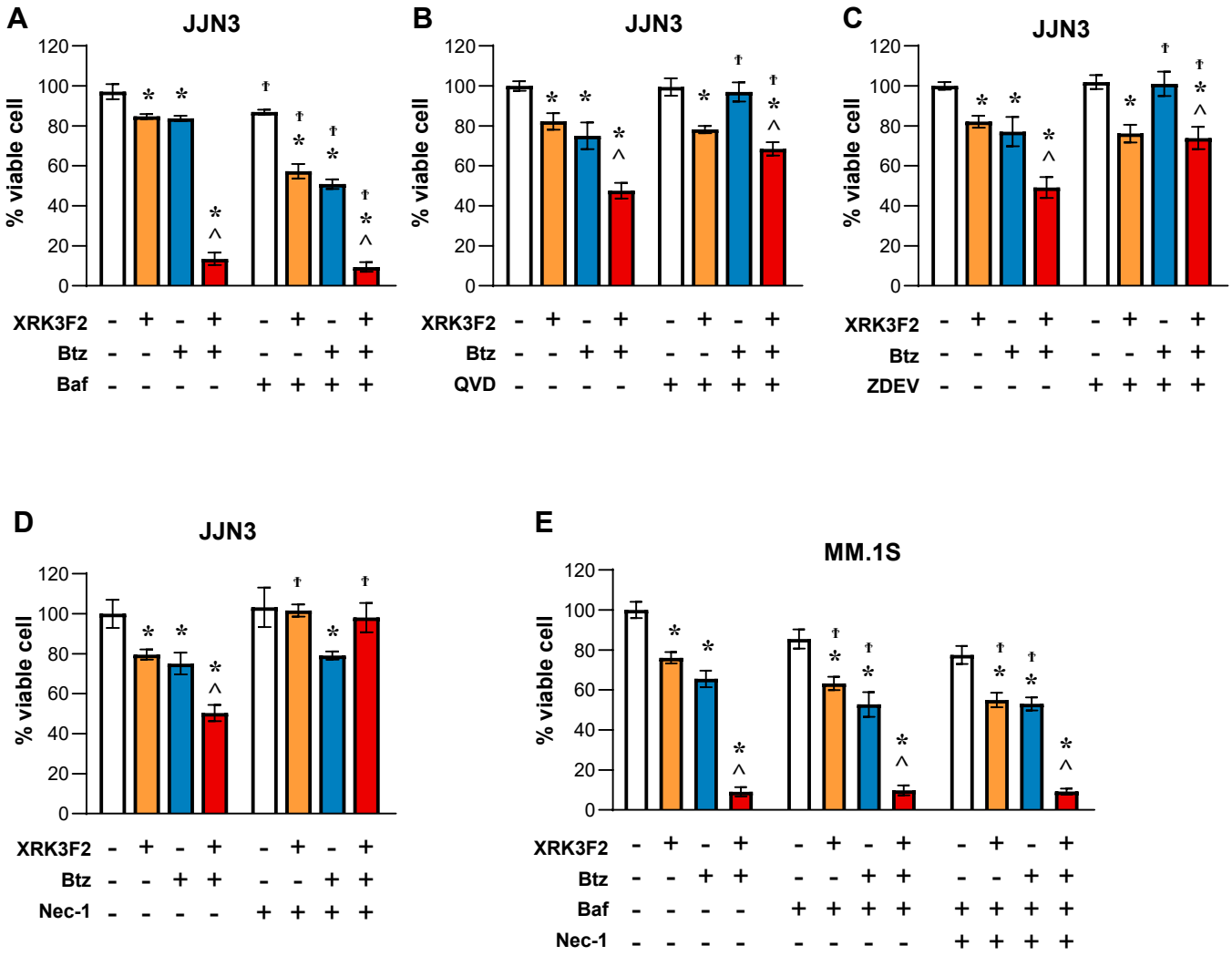

Supplementary Fig. 4. **XRK3F2 plus Bortezomib combination activates multiple death pathways and overcomes apoptosis resistance in JJN3.** JJN3 cells were treated with 5μM XRK3F2, 3nM Btz, or XRK3F2-Btz combination (5μM/3nM) for 24h hours in the presence or absence of Baf (40nM) (**A**), QVD (20μM) (**B**), Z-DEV (20μM) (**C**) Nec-1 (60μM) (**D**) or Baf (40nM) plus Nec-1 € Cell viability was evaluated using alamarBlue assays. Data are presented as bars, means±SD (n=4-6/group), and expressed as % of viable cells normalized versus vehicle-treated control. *p<0.05 vs vehicle, ^p<0.05 vs XRK3F2 or Btz alone, and † p<0.05 vs control vs Baf/QVD/ZDEV culture by two-way ANOVA with post hoc Bonferroni's correction.

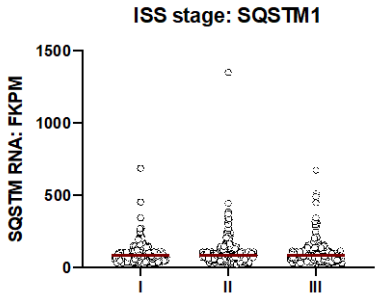

Tukey's multiple comparisons test	Mean Diff.	95.00% CI of diff.	Significant?	Summary	Adjusted P Value
I vs. II	-13.62	-30.94 to 3.697	No	ns	0.1551
I vs. III	-12.31	-30.83 to 6.220	No	ns	0.2638
II vs. III	1.316	-17.06 to 19.69	No	ns	0.9845

Supplementary Fig 5. p62 is highly expressed in MM patients CD138+ cells independent of the disease stages.

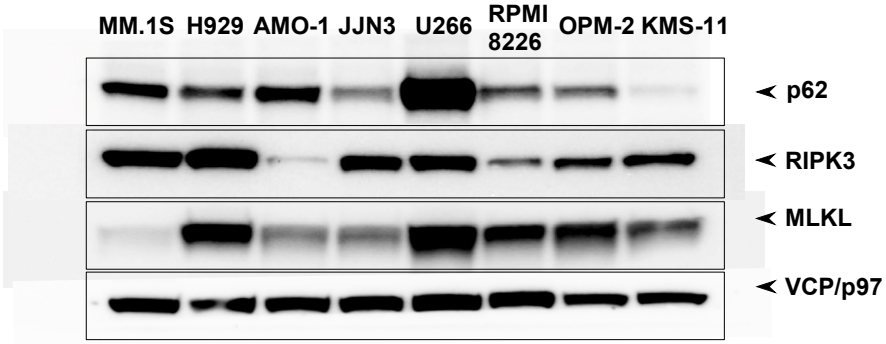

Supplementary Fig 6. p62, RIPK3 and MLKL expression in a panel of MM cell lines.

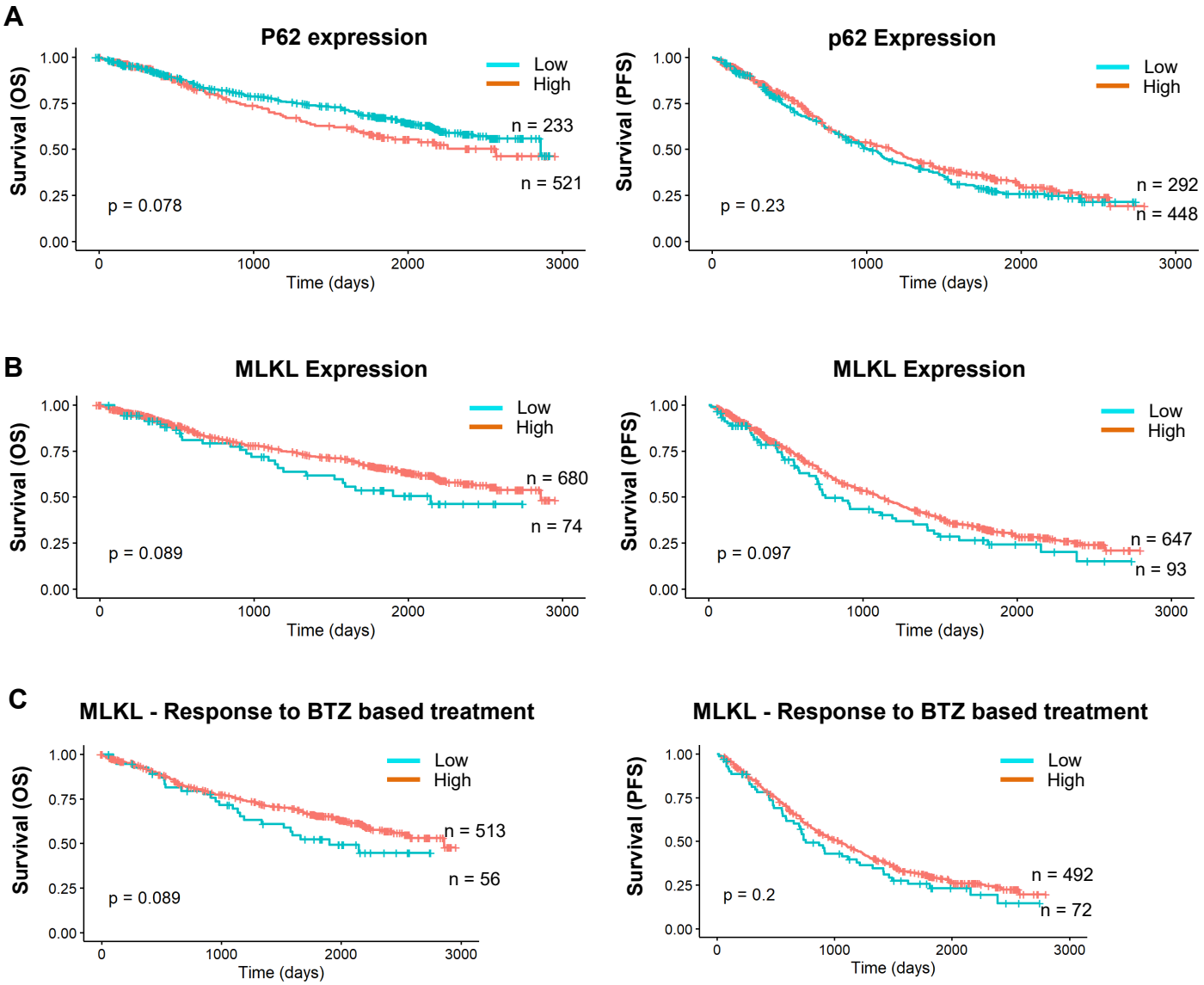

Supplementary Fig 7. **Impact of gene expression on overall survival (OS) and progression-free survival (PFS) in MM patients.** OS (left panel) and PFS (days, right panel) in patients with low and high **A** p62 mRNA expression or **B** MLKL mRNA expression. **C** OS (left panel) and OS (days, right panel) in response to Btz-based therapies in patients with high and low MLKL expression using MMRF CoMMpass (IA15) dataset.

Supplementary Methods, Tables and References

Chemicals. Cell culture media, penicillin and streptomycin were from Invitrogen. AlamarBlue® Cell Viability and Trypan blue assay kits were from ThermosFisher Scientific (Waltham, MA, USA). Caspase-3 Inhibitor Z-DEVD-FMK (# FMK004) and Pan Caspase Inhibitor Q-VD (#OPH001) were from R&D Systems (Minneapolis, MN); GSK'872 (#64920) and necrosulfonamide (#5025) were from Tocris Bioscience (Minneapolis, MN); Necrostatin-1 (#BML-AP309) was from Enzo Lifesciences (Farmingdale, NY); Bafilomycin A1 (#B1793) was from Sigma-Aldrich (Saint Louis, MO, USA). Bortezomib (Btz) (#S1013) was from Selleck Chemicals (Houston, TX). XRK3F2 was synthesized by a published route (1) and purified to greater than 97% purity by HPLC by the Chemical Genomics Core Facility at the Indiana University School of Medicine. F2 indicates the two fluorine atoms to increase stability *in vivo* added to the parental XRK3, which Cha-Molstad et al. (2) refer to as XIE62-1004.

Antibodies. Anti-SQSTM1/p62 (#ab155686), VCP (#ab11433) and human p-MLKL (#187,091) were from Abcam (Cambridge, MA); Cleaved Caspase-3 (#9664), Caspase-3 (#9662), Cleaved Caspase-8 (#9748), Caspase-8 (#4790), p-IκBα (#2859), IκBα (#9242), p-NFκB p65 (#3033) were from Cell Signaling Technology (Danvers, MA). Anti-RIP1 clone 38/RIP (# 610459) was from BD Biosciences (Franklin Lakes, NJ). Anti-RIP3 (#2283) was from ProSci (Poway, CA). Anti-MLKL (#MABC604) was from Merck Millipore (Burlington, MA). Anti-LC3B (#L7543), β-actin (#A5441) and α-tubulin (#T9026) as well as propidium iodide were from Sigma-Aldrich. Anti-NFκB p65 (#sc-8008), anti-RIP3 (sc-374639) were from Santa Cruz Biotechnology (Dallas, TX).

Apoptosis/Necroptosis. Apoptosis/Necroptosis ratio was assessed by 1) Quantitative Assessment by Flow using TACS Annexin V-FITC Apoptosis Detection Kit (#4830-250, R&D Systems) and flow cytometry detection (Fortessa flow cytometer, Becton Dickinson) as previously described

(3). Post-acquisition analysis of the gated cell subsets was performed using FlowJo software (Tree Star, OR). 2) Release of the enzyme lactate dehydrogenase (LDH) using Pierce LDH Cytotoxicity Assay Kit (#88953) as previously described (4).

Cell-to-cell co-cultures. Direct MM:HS5 cell-to-cell co-cultures were established by adding MM cells on top of HS5 cells in a 1:5 (HS5:MM) ratio. Co-cultures were treated with Btz (3nM) every 24h. In these co-cultures, MM cells were stained with the fluorescent cell-tracker DiI following the manufacturer's recommendations. Apoptosis in DiD+ MM cells was assayed by flow cytometry using the Annexin V apoptosis Detection kit (BD Biosciences) following the manufacturer's recommendations. Samples were analyzed in a BD FACSCalibur (UAMS Core Facility for Flow cytometry) within 1h. At least 10,000 cells were used for each group, and the data was analyzed by FlowJo software to detect different cell populations.

Immunoprecipitation and Western blotting. Cell pellets were lysed with IP lysis buffer containing 25 mM TRIS-HCl (pH7.4), 150 mM NaCl, 1 mM EDTA, 1% NP-40 and 5% glycerol, supplemented with proteinase inhibitor cocktail (#P8340, MilliporeSigma). Five hundred µg of lysates incubated with 2 µg anti-RIP1 (Clone 38/RIP; BD Bioscience) or control (mouse IgG2a) antibodies overnight at 4°C. Protein/antibody complexes were precipitated by protein A/G magnetic beads (Invitrogen) for 4h. Denatured protein complexes were separated by 10% SDS-PAGE gel electrophoresis and transferred to PVDF membrane. The immune complexes were subject to western blotting using anti-RIP1 (Clone 38/RIP; BD Bioscience) and anti-RIP3 (Prosci.Inc) primary antibodies and specific HRP-linked secondary antibodies, followed by visualization with enhanced chemiluminescence kit (Thermo Scientific). For the detection of phospho-MLKL, cell lysates were prepared in %SDS hot lysis buffer. Lysates were boiled (10 min; 95°C), sonicated (40kW, 3 seconds, intervals 3 seconds, 25-30 times) and the supernatant

obtained after centrifugation (17000g; 10 minutes) was subject to protein concentration followed by western blotting. For regular western blotting, protein lysates were extracted in RIPA lysis buffer (#sc-24948; SCB) supplemented with protease inhibitors cocktail (Millipore Sigma). Equal amounts of proteins, as determined by bicinchoninic acid assay protein analysis (Pierce), were separated on Any kD^{TM} SDS-PAGE gels (Bio-Rad Laboratories, Hercules, CA) and transferred onto PVDF membranes. For the detection of immune complexes, the membranes were incubated with various primary antibodies and specific HRP-linked secondary antibodies, which were detected using the enhanced chemiluminescence kit (Thermo Scientific). The immune complexes were quantified by densitometry using ImageJ software after normalization to specific loading controls.

Assessment of autophagy. During autophagy, the microtubule-associated protein 1A/1B-light chain 3 (LC3) is converted from LC3-I to the lipidated form LC3-II. Densitometric determination of the LC3-I/LC3-II ratio from Western blots provides and index of autophagic flux.

Mouse model of human MM. Immunodeficient 6-8 wk-old female SCID-CB17 mice (Fox Chase SCID beige CB17.Cg-PrkdcscidLystbg-J/Crl congenics) were purchased from Charles River and acclimated. Forty mice injected intratibially (IT) with $1x10^5$ human JJN3 myeloma cells in 20µl of PBS and an additional five with PBS alone. After three weeks, mouse sera was assayed by ELISA for human κ light chain to confirm tumor engraftment and limbs x-rayed by Faxitron under isoflurane inhalation anesthesia for presence of osteolytic bone lesions. Engrafted mice were randomized to four groups, then treated for two weeks with vehicle, XRK3F2, Btz or XRK3F2+Btz. The target sample size of 8 mice was calculated based on our previous study (5)**.** All treatments were 100µL of 15% hydroxylpropyl-β-cyclodextrin in saline, which was also used for delivery of XRK3F3 (insoluble in water or ethanol) at 27mg/kg, given IP daily Monday-Friday.

Bortezomib was freshly diluted in the same vehicle and injected subcutaneously twice a week for two weeks at 0.25 mg/kg. Serum was collected at euthanasia under isoflurane anesthesia and assayed by ELISA for human kappa light chain as marker of tumor burden. After preliminary analysis of each treatment group, mice showing light chain values greater than two standard deviations from the mean were excluded from the final analyses, leaving 7 or 8 mice per group.

Bone analyses Animal legs were analyzed by Faxitron X-ray, followed by removal of surrounding muscle and formalin fixation. Microcomputed x-ray tomography (μCT) scanning was performed to measure morphological indices of distal regions of tibiae (6). Images were acquired using a Bruker Skyscan 1176 with the following parameters: pixel size = 9 μm^3; peak tube potential = 50 kV; X-ray intensity = 500 μA; 0.3° rotation step. Raw images were reconstructed using SkyScan reconstruction software and analyzed using Skyscan CT Analyser software (CTAn; Bruker). Cortical bone of the injected legs was analyzed between 1 and 2 mm from the tibia-fibula junction using a threshold of 160–255. Trabecular bone of the contralateral leg was analyzed between 0.5 and 1.5 mm under the tibial proximal growth plate using a threshold of 80–255. After tomography, bones were decalcified in EDTA and embedded for routine histology.

ELISA. Human kappa light chain (E88-115, Bethyl Laboratories, Inc., Montgomery,TX), as a marker of myeloma tumor burden, and human high mobility group box 1 protein (HMGB1, # E88-115, Bethyl Laboratories).), as a marker of myeloma cell death (7) were determined in serum using enzyme-linked immunosorbent assays (ELISA) according to the manufacturer's instructions. Two markers of bone metabolism, mouse N-terminal propeptide of type I procollagen (P1NP, AC-33F1, a formation marker) and C-terminal telopeptides of type I collagen (CTX, AC-06F1, a marker of osteolysis), were likewise determined in serum by ELISAs.

Bioinformatic analyses of publicly available datasets. Gene expression data for RIPK3, RIPK1, SQSTM1 (p62), and MLKL were obtained from the MMRF Researcher Gateway using version IA18. Salmon count data were imported into R and normalized using DESeq2 (8). The optimal cutpoint for high and low gene expression groups was determined for each of the genes using the survminer (9) package in R, based on either progression-free survival (PFS) or overall survival (OS). The default method of the maximally selected rank statistics from the maxstat package was used for the optimal cutpoint algorithm selection method. The PFS and OS of bortezomib-treated and non-bortezomib-treated patients were compared within the context of high vs low expression of RIPK3, RIPK1, SQSTM1 (p62), and MLKL, based on the optimal cutpoint. Kaplan-Meier survival curves were generated using the survival and survminer packages in R using the ggsurvplot function.

Real-time RT-PCR (qPCR). Total mRNA was extracted using RNeasy (QIAGEN, Germantown MD) per the manufacturer's protocol and reverse-transcribed using High-capacity cDNA reverse transcription kit (Applied Biosystem) on a T100 Thermal Cycler (Bio-Rad Laboratories). Quantitative PCR was performed on an CFX96 Real-Time System (Bio-Rad Laboratories) using a SsoAdvanced SYBR Green Supermix (Bio-Rad Laboratories) and cDNA equivalent to 40 ng RNA in a 10 µl reaction according to the manufacturer's instructions. The DNA sequences of primers used for qPCR are listed in Supplemental Table S3. Relative expression was calculated using the comparative $2^{-\Delta\Delta Ct}$ method, with 18S rRNA used as a housekeeping gene.

Supplementary Table 1: MM cell lines IC50

MM cell lines IC50	XRK3F2 (μM)	Btz (nM)
MM.1S t(14;16) t(8,14)	7.9	4.2
NCI-H929 t(4;14);	9.4	5.3
RPMI8226 t(8,22); t(16,22)	14.35	12.78
JJN3 t(14;16); t(8,14)	20.5	17.2
U266 t(11;14)	7	15.62
KMS11 t(4;14)	13.5	21.5

Supplementary Table 2: **Main characteristics of the US patient cohort**

Patient ID	***Clinical features***					
	Age (years)	***Clinical status***	***ISS Stage***	***Treatment received***	***Auto SCT***	***Histologic Type***
MM 1	75	New diagnosis	2	Btz/Dexa	No	IgG kappa MM
MM 2	59	Refractory/Relapsed	3	Btz/Mp	Yes	IgG kappa MM
MM 3	76	Refractory/Relapsed	n/a	Melph/Pred	No	IgG kappa MM
MM 4	70	Refractory/Relapsed	n/a	Btz/Lena	Yes	IgG kappa MM
MM 5	67	Refractory/Relapsed	3	Btz/Lena/Pred	No	IgG kappa MM
MM 6	48	New diagnosis	1	Lena/Dexa/Carfil/Poma/ Dara/Cyc	Yes	IgG kappa MM
MM 10	46	Refractory/Relapsed	2	Thal/Dexa	Yes	IgG kappa MM
MM 11	68	Refractory/Relapsed	2	Melp/Lena	Yes	IgG kappa MM
MM 12	64	Refractory/Relapsed	2	Lena/Btz/Dexa/Thal	Yes	IgG kappa MM
MM 13	67	New diagnosis	n/a	Melph/Ixa	Yes	AL Amyloidosis
MM 14	60	Refractory/Relapsed	2	Carfil/Dexa/Cyc/ Pred/Btz/Benda	Yes	IgG lambda MM

Supplementary Table 3: Sequences of qPCR primers used for amplification of human (A) and mouse (B) mRNA

A. Human

SQSTM1/p62	Forward	CGGCTGATTGAGTCCCTCTC
	Reverse	GCCGCTCCGATGTCATAGTT

B. Mouse

Gene	Primer	Sequence 5'-3'
Runx2	Forward	AGGGACTATGGCGTCAAACA
	Reverse	AGAAGCTTTGCTGACACGGT
Osterix	Forward	AGAGGTTCACTCGCTCTGACGA
	Reverse	TTGCTCAAGTGGTCGCTTCTG
ATF4	Forward	TCGGCCCAAACCTTATGACC
	Reverse	TGGCTGCTGTCTTGTTTTGC

REFERENCES

1. Xie X-Q RG, Myint K-Z, Kurihara N; US Patent 2017. P62-ZZ CHEMICAL INHIBITORUS9580382B2.
2. Cha-Molstad H, Yu JE, Feng Z, Lee SH, Kim JG, Yang P*, et al.* p62/SQSTM1/Sequestosome-1 is an N-recognin of the N-end rule pathway which modulates autophagosome biogenesis. Nat Commun **2017**;8:102
3. Shlomovitz I, Zargarian S, Erlich Z, Edry-Botzer L, Gerlic M. Distinguishing Necroptosis from Apoptosis. Methods Mol Biol **2018**;1857:35-51
4. Chan FK, Moriwaki K, De Rosa MJ. Detection of necrosis by release of lactate dehydrogenase activity. Methods Mol Biol **2013**;979:65-70
5. Teramachi J, Silbermann R, Yang P, Zhao W, Mohammad KS, Guo J*, et al.* Blocking the ZZ domain of sequestosome1/p62 suppresses myeloma growth and osteoclast formation in vitro and induces dramatic bone formation in myeloma-bearing bones in vivo. Leukemia **2016**;30:390-8
6. Campbell GM, Sophocleous A. Quantitative analysis of bone and soft tissue by micro-computed tomography: applications to ex vivo and in vivo studies. Bonekey Rep **2014**;3:564
7. Nakano H, Murai S, Moriwaki K. Regulation of the release of damage-associated molecular patterns from necroptotic cells. Biochem J **2022**;479:677-85
8. Love MI, Huber W, Anders S. Moderated estimation of fold change and dispersion for RNA-seq data with DESeq2. Genome Biol **2014**;15:550
9. Alboukadel Kassambara MK, Przemyslaw Biecek. 2021 survminer: Drawing Survival Curves using 'ggplot2'. R package version 0.4.9. <https://CRAN.R-project.org/package=survminer.>.